COHERENCE FROM SASE

Investigation of Longitudinal Pulse Shaping at SPARC

Time-domain measurement of single-spike radiation produced from a self-amplified spontaneous emission free-electron laser using an energy-chirped electron beam and a tapered undulator

GABRIEL MARCUS

Particle Beam Physics Laboratory

University of California, Los Angeles

LBNL

April 20, 2012

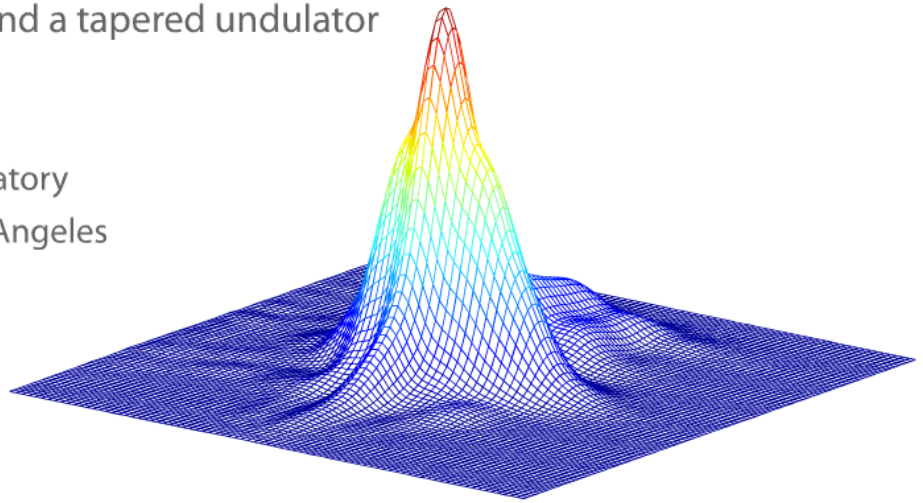

UCLA

- Motivation
- Brief FEL overview
- Description of the Experiment
- Experimental Results
  - Time Domain Measurement
  - FROG
- Conclusions

Motivation

- Desire to probe and understand nature
- Control matter at the level of
  - Atoms
  - Electrons
  - Spins
- Requires tools to reach into regions of higher resolution
  - Spatial
  - Temporal
  - Energy
- Study materials at time and length scales of atomic and electronic motion

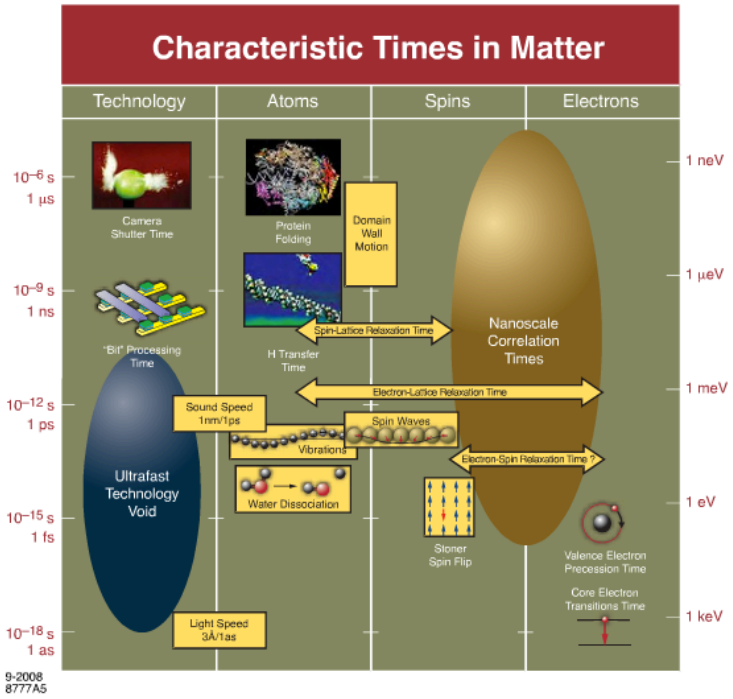
Characteristic Times in Matter
Technology
Atoms
Spins
Electrons
10−6 s
1 µs
10−9 s
1 ns
10−12 s
1 ps
10−15 s
1 fs
10−18 s
1 as
1 neV
1 µeV
1 meV
1 eV
1 keV
Camera Shutter Time
"Bit" Processing Time
Ultrafast Technology Void
Light Speed 3Å/1as
Protein Folding
Domain Wall Motion
H Transfer Time
Spin-Lattice Relaxation Time
Nanoscale Correlation Times
Electron-Lattice Relaxation Time
Sound Speed 1nm/1ps
Spin Waves
Vibrations
Electron-Spin Relaxation Time ?
Water Dissociation
Stoner Spin Flip
Valence Electron Precession Time
Core Electron Transitions Time
9-2008
8777A5

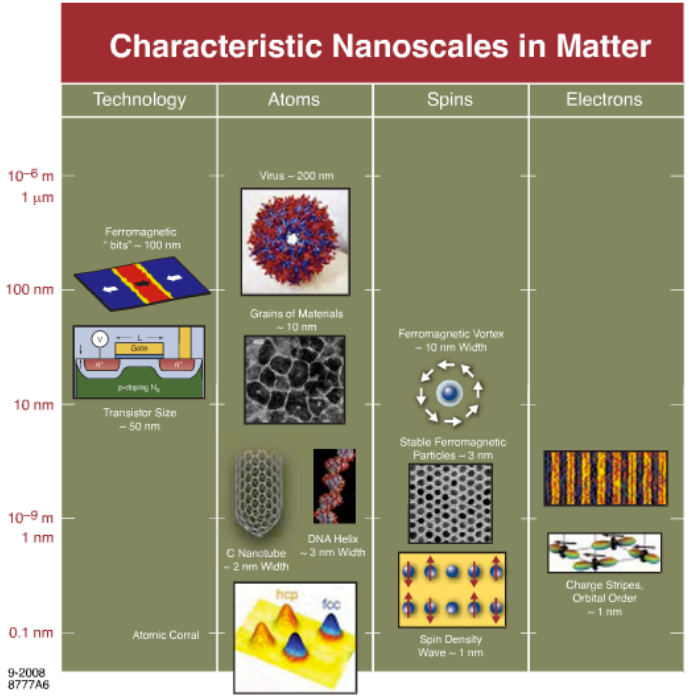
Characteristic Nanoscales in Matter
Technology
Atoms
Spins
Electrons
10−6 m
1 µm
100 nm
10 nm
10−9 m
1 nm
0.1 nm
Ferromagnetic "bits" ~ 100 nm
Transistor Size ~ 50 nm
Atomic Corral
Virus ~ 200 nm
Grains of Materials ~ 10 nm
C Nanotube ~ 2 nm Width
DNA Helix ~ 3 nm Width
hcp
fcc
Ferromagnetic Vortex ~ 10 nm Width
Stable Ferromagnetic Particles ~ 3 nm
Spin Density Wave ~ 1 nm
Charge Stripes, Orbital Order ~ 1 nm
9-2008
8777A6

LBNL-1090E

Science Drivers

- Chemical reactivity
  - Studying catalysis, combustion and other far-from-equilibrium processes
- Atoms to materials
  - Study the emergence of solid-state properties from collections of atoms
- Matter in extreme conditions
  - Study plasmas, geological sciences, laboratory astrophysics
- Hierarchical biology
  - Study spatial-temporal dynamics and phase transitions

New X-Ray Requirements

- Control of the longitudinal phase space
  - Control of pulse shape, amplitude and phase
- Transverse coherence
  - Diffractive imaging
- High average photon flux
  - Short pulses with high rep rate
- Control of polarization and wavelength
  - Extend energy range to 100keV

Hybrid time-frequency domain

Recurring themes of ultra-short, longitudinally coherent pulses require sophisticated pulse visualization and reconstruction method

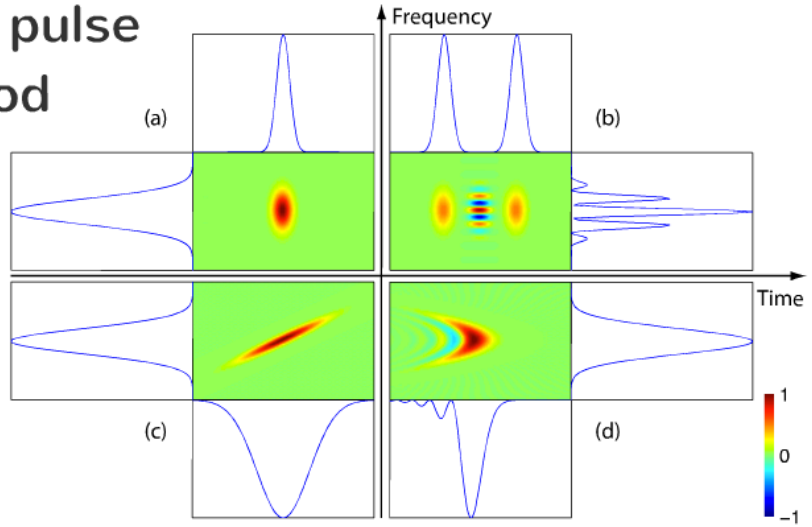

Wigner Distribution

$$W(t,\omega) = \frac{1}{2\pi}\int_{-\infty}^{\infty} E^*(t-\frac{\tau}{2})E(t+\frac{\tau}{2})e^{-i\tau\omega}\mathrm{d}\tau$$

Cohen Class

$$C(t,\omega) = \frac{1}{4\pi^2}\int_{-\infty}^{\infty}\int_{-\infty}^{\infty}\int_{-\infty}^{\infty} E^*(u-\frac{\tau}{2})E(u+\frac{\tau}{2})K(\theta,\tau)e^{-i\theta t-i\tau\omega+i\theta u}\mathrm{d}u\mathrm{d}\tau\mathrm{d}\theta$$

Gabor Spectrogram

aka - short-time Fourier transform

$$S(\tau,\omega) = \left| \frac{1}{\sqrt{2\pi}} \int_{-\infty}^{\infty} E(t) g(t-\tau) e^{-i\omega t} \mathrm{d}t \right|^2$$

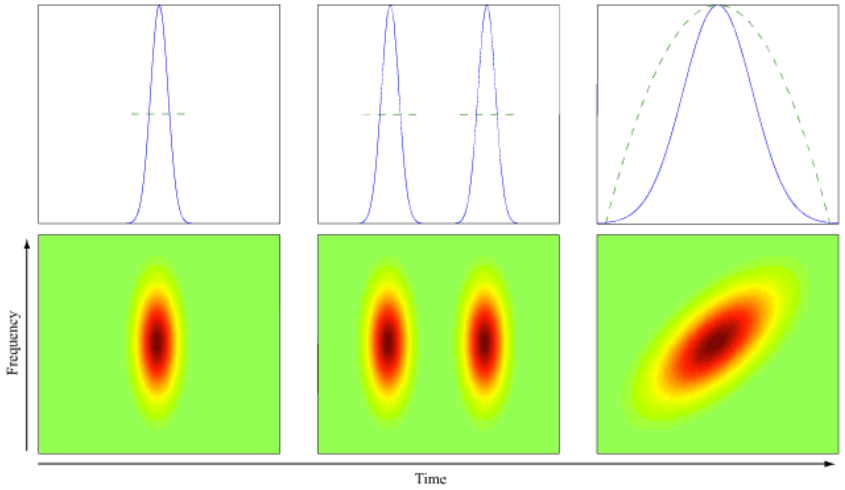

This distribution is positive definite and can be measured by square-law detectors (photodiodes)

- Motivation
- Brief FEL overview
- Description of the Experiment
- Experimental Results
- Time Domain Measurement
- FROG
- Conclusions

Basic Concepts

- FELs convert the kinetic energy of an e-beam to EM radiation
- Central components
  - E-beam: Lasing/gain medium
    - Charge
    - Energy
    - Emittance
  - Undulator: Couples e-beam to EM radiation
    - Magnetic field
    - Period
    - Length
  - EM radiation: Amplified signal
    - Tuned according to resonance
    - Different coherence properties depending on operational mode
      - Seeded vs. SASE

Undulator radiation

- Magnetic field wiggles the electrons

$$B_y(z) = B_0 \sin(k_u z), k_u = \frac{2\pi}{\lambda_u}$$

- Resonance condition

$$\lambda_r = \frac{\lambda_u}{2\gamma^2}\left(1 + \frac{K^2}{2} + \gamma^2\psi^2\right), K = \frac{eB_0}{mck_u}$$

- EM wave in forward direction copropagates with the e-beam

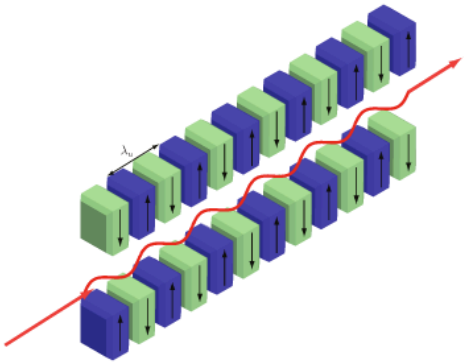

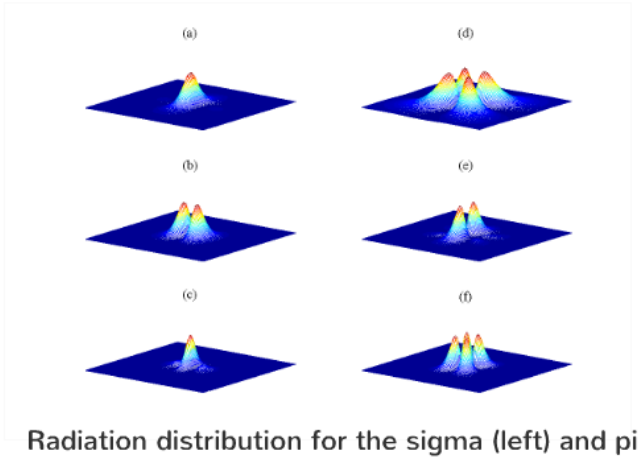

Radiation distribution for the sigma (left) and pi (right) mode polarizations in the first three harmonics for single particle motion.

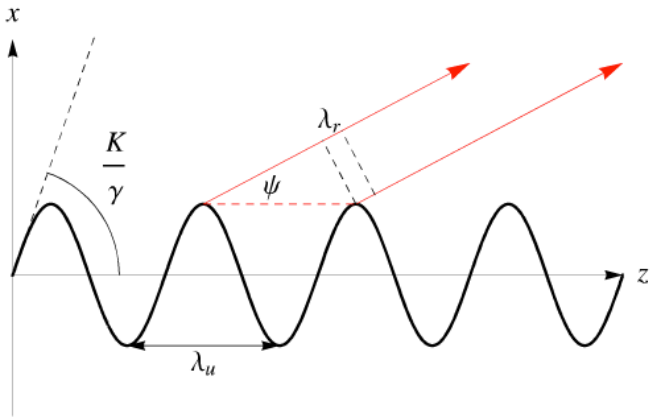

FEL interaction

- Resonant free space interaction of EM wave and e-beam is not sustained

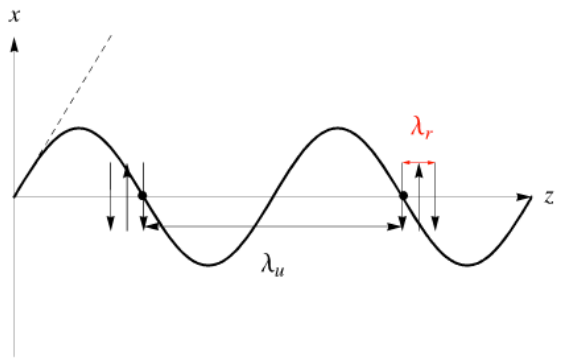

- Slippage in the undulator allows for a resonant interaction and energy can efficiently be exchanged

- e-beam becomes microbunched
  - Emits coherent radiation
    - Amplify the EM signal at the expense of the e-beam kinetic energy

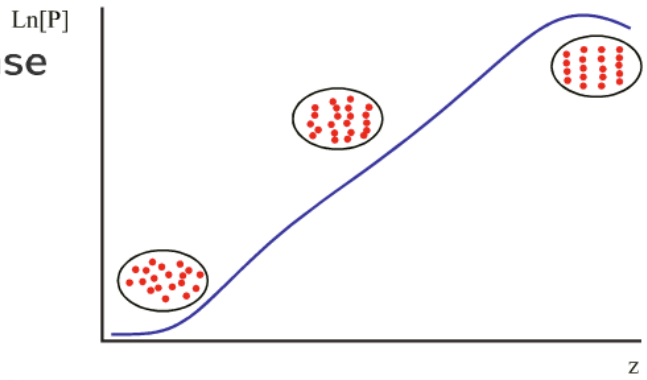

- Saturation
  - Resonance condition is interrupted
  - Microbunching is maximized
  - Energy spread in e-beam covers the FEL bandwidth

FEL analysis: 1-D Linearized Vlasov-Maxwell equations

- The pendulum equations describe the motion of electrons in the ponderomotive potential due to the combined undulator and radiation fields

$$\frac{\mathrm{d}\theta}{\mathrm{d}z} = 2k_u\eta \qquad \frac{\mathrm{d}\eta}{\mathrm{d}z} = -\kappa_1 E\sin(\theta)$$

$$\theta = (k+k_u)\,z - \omega t \qquad \eta = \frac{\gamma-\gamma_R}{\gamma_R}$$

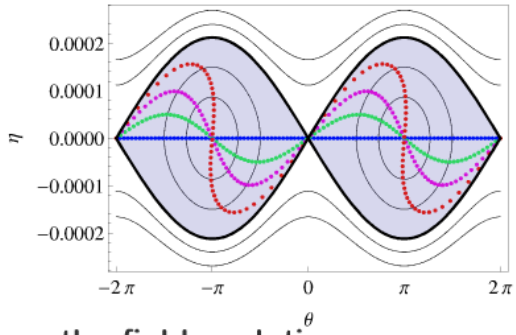

- The Maxwell equations can be combined to produce the field evolution equation in the frequency domain where the electron distribution function is governed by the Vlasov equation

$$\left(\frac{\partial}{\partial z} + i\Delta\nu k_u\right) A(z,\nu) = -\kappa_2 n_0 \int_{-\infty}^{\infty} F(\nu,\eta;z)\mathrm{d}\eta, \quad \frac{\mathrm{d}}{\mathrm{d}z}F(\theta,\eta;z) = \frac{\partial F}{\partial z} + \frac{\partial F}{\partial\theta}\frac{\partial\theta}{\partial z} + \frac{\partial F}{\partial\eta}\frac{\partial\eta}{\partial z} = 0.$$

- These equations can be solved via the Laplace transform, producing an exponentially growing field for a cold beam

$$E\,(z,t) \propto e^{\sqrt{3}\rho k_u z}\sum_{j=1}^{N_e} exp\left[-\frac{\left(t-t_j-\frac{z}{v_g}\right)^2}{4\sigma_\tau^2}\left(1+\frac{i}{\sqrt{3}}\right)\right]$$

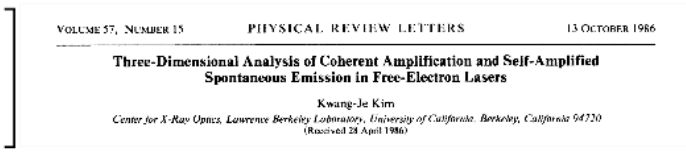
VOLUME 57, NUMBER 15 PHYSICAL REVIEW LETTERS 13 OCTOBER 1986

Three-Dimensional Analysis of Coherent Amplification and Self-Amplified Spontaneous Emission in Free-Electron Lasers

Kwang-Je Kim
Center for X-Ray Optics, Lawrence Berkeley Laboratory, University of California, Berkeley, California 94720
(Received 28 April 1986)

FEL characteristics

- The growth rate of the exponentially growing mode is determined by the roots of the FEL dispersion relation

$$\Omega(\mu) = \mu - \frac{\Delta\nu}{2\rho} + \rho \int_{-\infty}^{\infty} \frac{\frac{\partial F_{0,\nu}}{\partial \eta}}{\mu - \frac{\eta}{\rho}} \mathrm{d}\eta$$

- Exponentially growing root, cold beam

$$F_{0,\nu}(\eta) = \delta(\eta) \qquad \mu_I = \frac{\sqrt{3}}{2} - \frac{\Delta\nu^2}{24\rho^2\sqrt{3}}$$

- Determines FEL characteristics

$$e^{4\rho k_u u_I z} = e^{\frac{z}{L_G}} e^{-\frac{1}{2}\left(\frac{\omega-\omega_m}{\omega_m \sigma_\nu}\right)^2}$$

$$L_G = \frac{\lambda_u}{4\pi\sqrt{3}\rho} \qquad \sigma_\nu = \sigma_{\Delta\omega/\omega} = \sqrt{\frac{3\sqrt{3}}{k_u z}\rho}$$

- Universal scaling parameter

$$\rho = \left(\frac{e^2 K^2 [JJ]^2 n_e}{32\epsilon_0 \gamma_R^3 m c^2 k_u^2}\right)^{\frac{1}{3}}$$

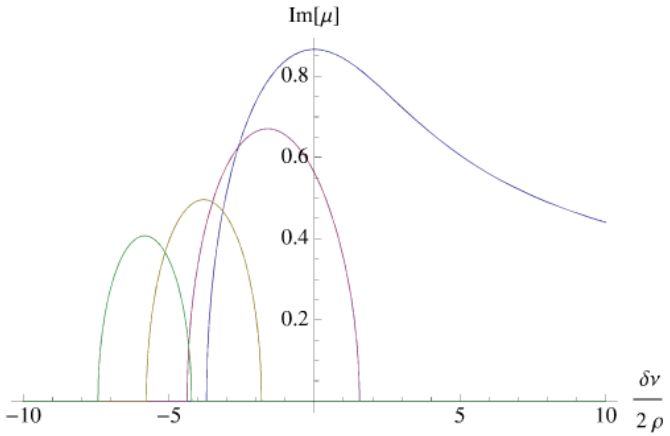

Growth rate as a function of detuning for a flattop energy distribution of different widths

- Saturation length: $L_s \sim \frac{\lambda_u}{\rho}$
- Output power: $P_s \sim \rho I_{beam} E_{beam}$
- Frequency bandwidth: $\frac{\Delta\omega}{\omega} \sim \rho$

Examples of SASE with low charge, high brightness beams in a short period, high field cryogenic undulator

TABLE I. Summary of the results of the GENESIS free electron laser simulations.

		SPARX		LCLS		$(T)^3$ FEL
E	GeV	2.1	4.5	13.65	13.65	1.74
I	kA	0.7	0.35	0.35	8.0	160
Q	pC	1.0	0.25	0.25	20	1600
$\epsilon_{n,x(y)}$	10^{-8} mrad	7.5(3.3)	3.3(3.3)	3.3(3.3)	40(14)	100(100)
λ_r	Å	6.5	1.4	0.15	0.15	9.5
$\bar{\beta}$	m	2.0	4.8	4.8	4.8	4.3
ρ	10^{-3}	1.8	0.75	0.36	0.51	3.6
L_{sat}	m	10	15	40	170	3
Output power	GW	2.4	4.5	2.4	1.0	1090

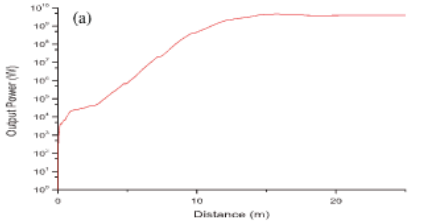

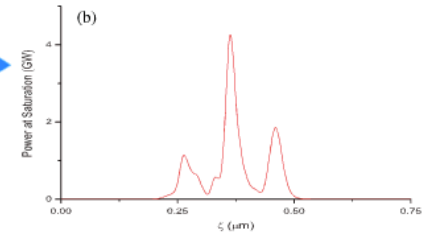

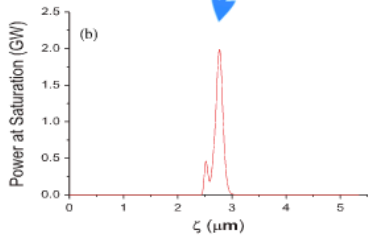

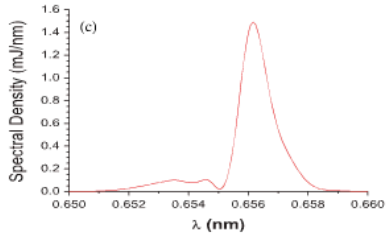

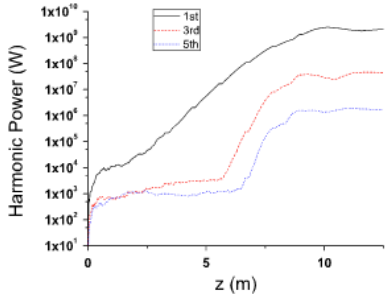

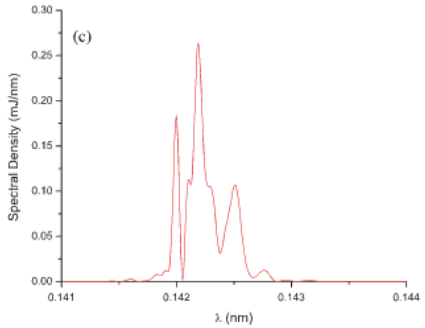

PHYSICAL REVIEW SPECIAL TOPICS - ACCELERATORS AND BEAMS **13**, 070702 (2010)

Short period, high field cryogenic undulator for extreme performance x-ray free electron lasers

F. H. O'Shea,[1,*] G. Marcus,[1] J. B. Rosenzweig,[1,†] M. Scheer,[2] J. Bahrdt,[2] R. Weingartner,[3] A. Gaupp,[2] and F. Grüner[3]
[1]*Department of Physics, University of California, Los Angeles, California 90095, USA*
[2]*Helmholtz-Zentrum Berlin für Materialien und Energie, 14109 Berlin, Germany*
[3]*Department of Physics, Ludwig-Maximilians-Universität, 85748 Garching, Germany*
(Received 9 March 2010; published 13 July 2010)

- Motivation
- Brief FEL overview
- Description of the Experiment
- Experimental Results
  - Time Domain Measurement
  - FROG
- Conclusions

Experimental layout

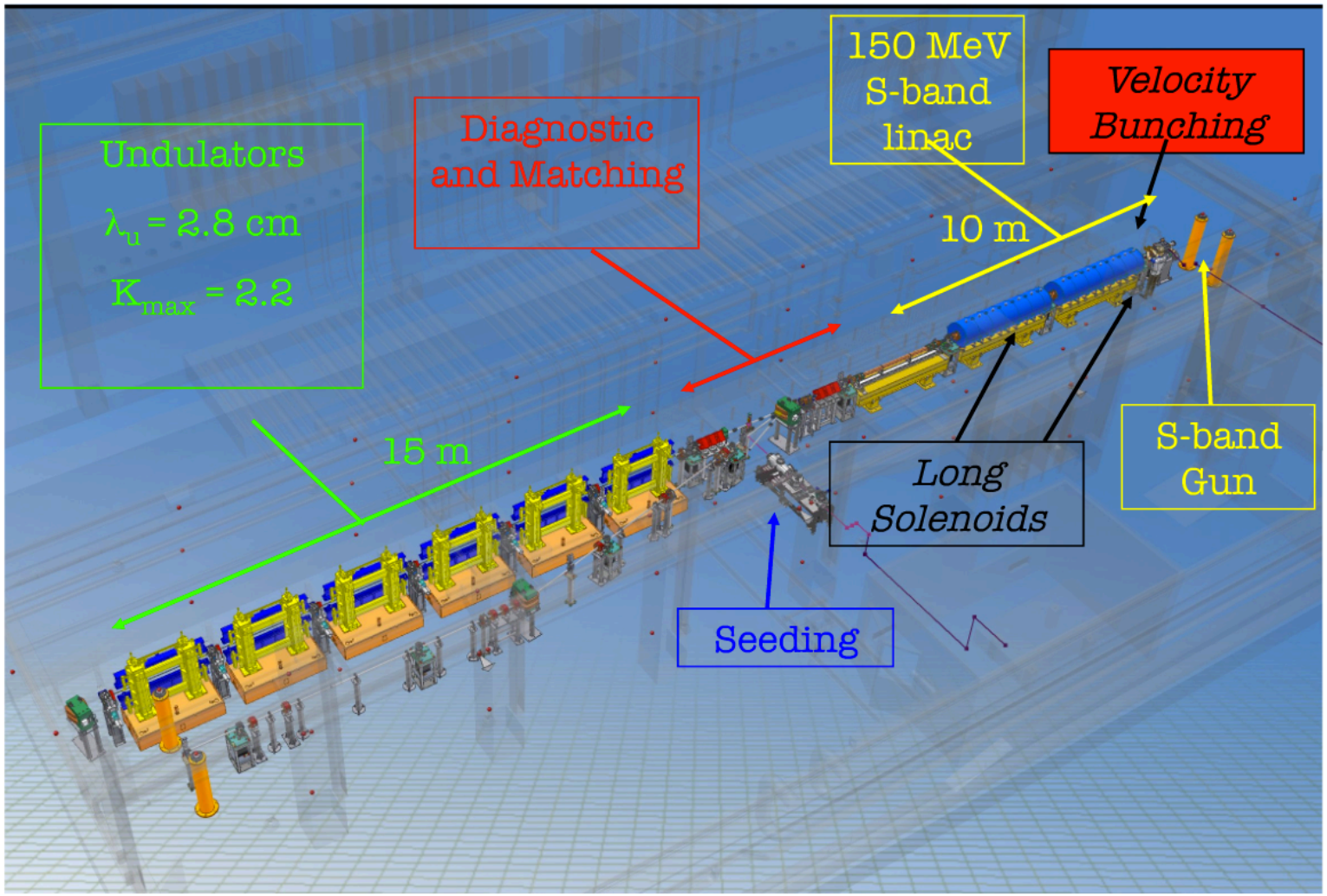

SPARC gun

- The RF gun is a 1.6 cell S-band BNL/UCLA/SLAC type
- Supports high field
  - ~10 MW power, ~120 MV/m on axis field
- e-beam energy parameters
  - energy ~5.6 MeV
  - current ~60 A
  - emittance ~1-2 mm-mrad
- Need to compress to increase the current
  - RF compressor: Velocity bunching

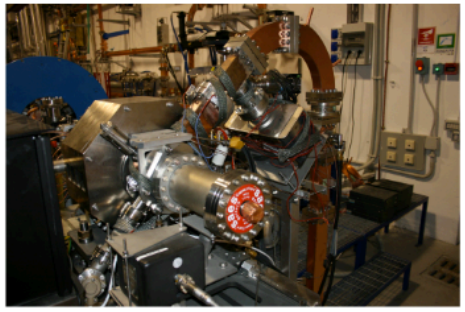

Velocity bunching - I

- Inject the e-beam into the long RF structure at the zero crossing field phase
- The beam will slip back to a phase where the field is accelerating
- The tail of the beam gains more energy than the head
- The beam develops an energy chirp and compresses
- Compression and acceleration are acheived simultaneously within the same linac section

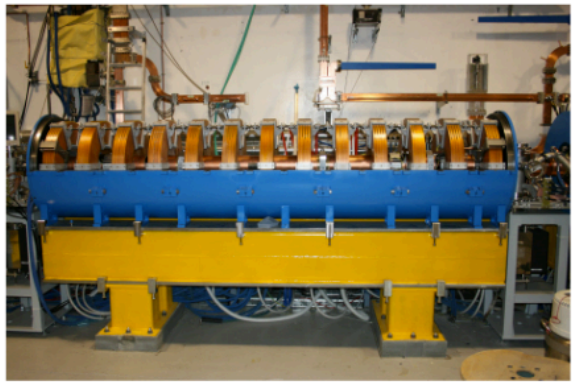

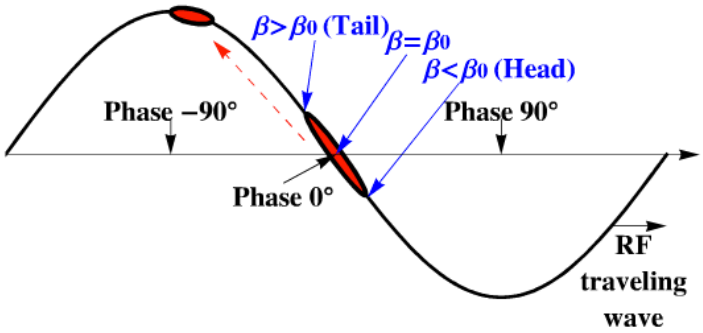

Velocity bunching - II

- **RF Wave:**

$$E_z = E_0 \sin(kz - \omega t + \phi_0)$$

- **Time-independent Hamiltonian:**

$$H = \gamma - \sqrt{\gamma^2 - 1} - \alpha \cos(\phi)$$

$$\alpha = eE_0/mc^2k$$

- **Equations of motion:**

$$\frac{\mathrm{d}\gamma}{\mathrm{d}z} = -\alpha k \sin(\phi)$$

$$\frac{\mathrm{d}\phi}{\mathrm{d}z} = k\left[1 - \frac{\gamma}{\sqrt{\gamma^2 - 1}}\right]$$

- **Limitations:**

$$\Delta\phi_\infty = f(\Delta\gamma_0, \Delta\phi_0)$$

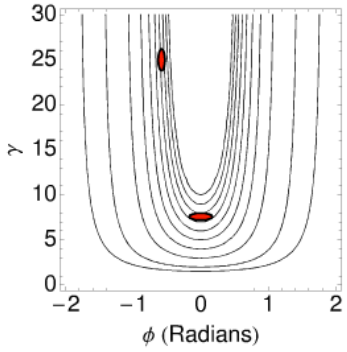

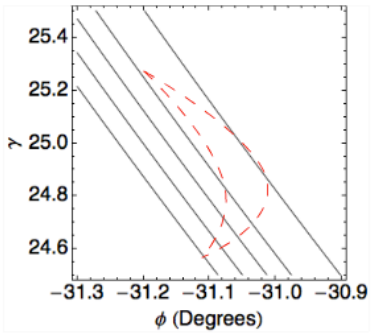

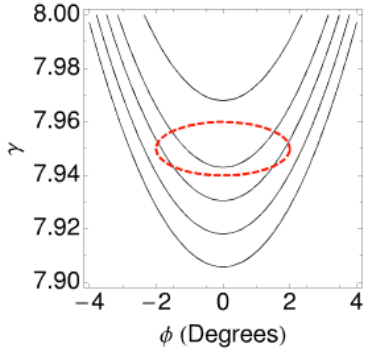

PHYSICAL REVIEW SPECIAL TOPICS - ACCELERATORS AND BEAMS **8**, 014401 (2005)

Velocity bunching of high-brightness electron beams

S. G. Anderson,[1,*] P. Musumeci,[2] J. B. Rosenzweig,[2] W. J. Brown,[1] R. J. England,[2] M. Ferrario,[3] J. S. Jacob,[1] M. C. Thompson,[2] G. Travish,[2] A. M. Tremaine,[1] and R. Yoder[2]

PHYSICAL REVIEW SPECIAL TOPICS - ACCELERATORS AND BEAMS **14**, 092804 (2011)

Phase space analysis of velocity bunched beams

D. Filippetto,* M. Bellaveglia, M. Castellano, E. Chiadroni, L. Cultrera, G. Di Pirro, M. Ferrario, L. Ficcadenti, A. Gallo, G. Gatti, E. Pace, C. Vaccarezza, and C. Vicario
INFN-LNF, Via E. Fermi, 40, 00044 Frascati, Rome, Italy

PRL **104**, 054801 (2010) PHYSICAL REVIEW LETTERS week ending 5 FEBRUARY 2010

Experimental Demonstration of Emittance Compensation with Velocity Bunching

M. Ferrario,[1] D. Alesini,[1] A. Bacci,[3] M. Bellaveglia,[1] R. Boni,[1] M. Boscolo,[1] M. Castellano,[1] E. Chiadroni,[1] A. Cianchi,[2] L. Cultrera,[1] G. Di Pirro,[1] L. Ficcadenti,[1] D. Filippetto,[1] V. Fusco,[1] A. Gallo,[1] G. Gatti,[1] L. Giannessi,[4] M. Labat,[4] B. Marchetti,[5] C. Marrelli,[1] M. Migliorati,[3] A. Mostacci,[3] E. Pace,[1] L. Palumbo,[3] M. Quattromini,[4] C. Ronsivalle,[4] A. R. Rossi,[5] J. Rosenzweig,[6] L. Serafini,[5] M. Serluca,[6] B. Spataro,[1] C. Vaccarezza,[1] and C. Vicario[1]

Energy-chirped e-beam and undulator taper

- Velocity bunching imparts an energy chirp on the e-beam
  - Linear chirp: $\gamma(s) = \gamma(s_0) + \alpha(s - s_0)$

$$\gamma(z) = \gamma_0 + \alpha z \frac{\lambda_0}{\lambda_u}\eta$$

- In absence of undulator taper, light exits the gain bandwidth when slips forward in the beam frame a distance:

$$\delta s \sim \frac{\rho\gamma_0}{\alpha}$$

- The taper that preserves the desired resonance condition is (from the resonance condition):

$$K(z) = 2\sqrt{\left(\gamma_0 + \alpha z \eta \frac{\lambda_0}{\lambda_u}\right)^2 \frac{\lambda_0}{\lambda_u} - \frac{1}{2}}$$

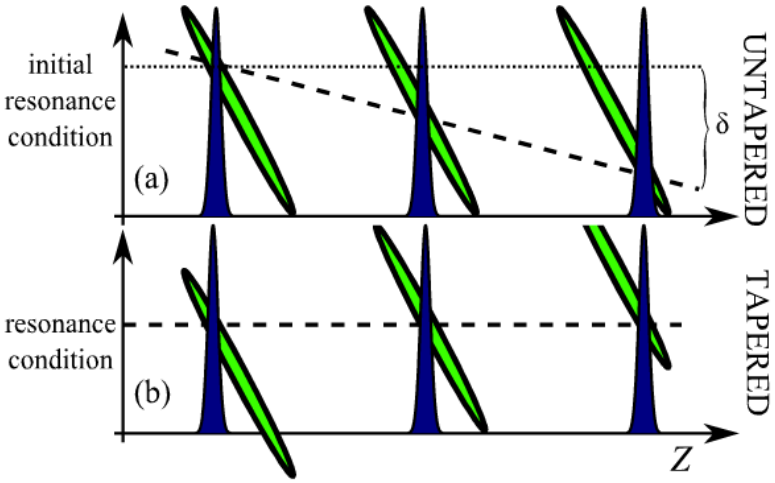

PRL 106, 144801 (2011) PHYSICAL REVIEW LETTERS week ending 8 APRIL 2011

Self-Amplified Spontaneous Emission Free-Electron Laser with an Energy-Chirped Electron Beam and Undulator Tapering

L. Giannessi,[1,*] A. Bacci,[2,4] M. Bellaveglia,[2] F. Briquez,[10] M. Castellano,[2] E. Chiadroni,[2] A. Cianchi,[8] F. Ciocci,[1] M. E. Couprie,[10] L. Cultrera,[2] G. Dattoli,[1] D. Filippetto,[2] M. Del Franco,[1] G. Di Pirro,[2] M. Ferrario,[2] L. Ficcadenti,[2] F. Frassetto,[6] A. Gallo,[2] G. Gatti,[2] M. Labat,[10] G. Marcus,[9] M. Moreno,[5] A. Mostacci,[5] E. Pace,[2] A. Petralia,[1] V. Petrillo,[3,4] L. Poletto,[6] M. Quattromini,[1] J. V. Rau,[7] C. Ronsivalle,[1] J. Rosenzweig,[9] A. R. Rossi,[2,4] V. Rossi Albertini,[7] E. Sabia,[1] M. Serluca,[5] S. Spampinati,[11] I. Spassovsky,[1] B. Spataro,[2] V. Surrenti,[1] C. Vaccarezza,[2] and C. Vicario[2]

- Motivation
- Brief FEL overview
- Description of the Experiment
- Experimental Results
  - Time Domain Measurement
  - FROG
- Conclusions

Chirp/taper results - spectral domain I

Parameter	Symbol	Value
charge	Q	400 pC
current	I	380 A
e-beam energy	E	115.2 MeV
e-beam energy chirp	α	-8.7 keV/μm
rms slice energy spread	σ_γ	6×10^{-3} (Max)
normalized x(y) emittance	$\epsilon_{n,x(y)}$	2.7(3.0) mm-mrad
undulator period	λ_u	2.8 cm
nominal radiation wavelength	λ	540 nm

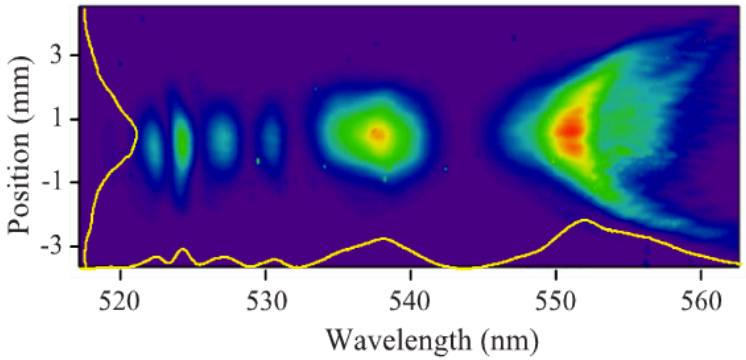

Single shot spectrum aquired with all undulators set at the nominal resonance of 540 nm. The strong e-beam chirp produces a broadband spectrum. The following quantities were averaged over 100 shots:

$$E = 7.8 \pm 8\mu J \qquad \lambda_0 = 537 \pm 5nm$$

$$\sigma_{\lambda,rms} = 8.8 \pm 2nm$$

Resonant frequency for a 115.2 MeV e-beam in the six undulators.

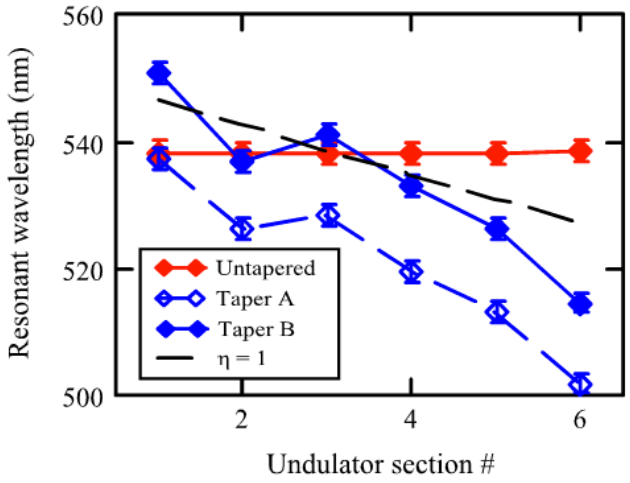

In order to compensate for the e-beam energy chirp, each undulator was progressively tuned, starting with the first, while minimizing the spectral width.

Taper B is after compensation of an observed wavelength blueshift. Discrepencies in Taper B and black curve arise because of nonlinearities in the energy chirp. Also, the taper simultaneously compensates for electron energy loss to the field.

Chirp/taper results - spectral domain II

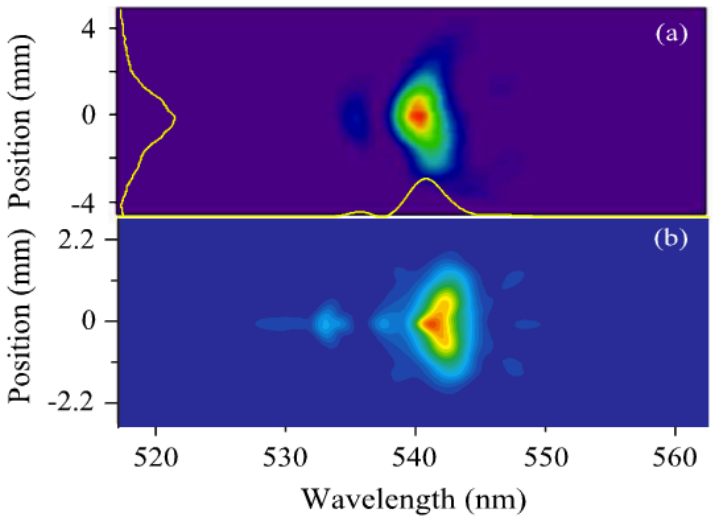

˜50% of the aquired spectra in the chirp/taper scenario exhibited exhibited single-spike behavior (above). Typical SASE spikes are absent and the spectrum is concentrated in a single coherence region. Experimental measurements (a) agree well with results from GENESIS (b), where the simulated data was processed to model the spectrometer input slit and grating transformations.

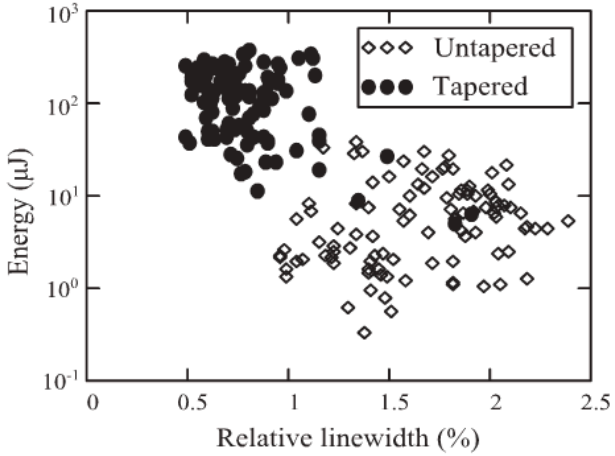

Energy vs relative spectral width for the untapered and tapered cases. Analysis of 100 spectra in the tapered case produces:

$$E = 139 \pm 97 \mu J$$

$$\sigma_{\lambda,rms} = 4.3 \pm 1.3 nm$$

While the number of 'single-spike' events in simulation (˜30%) was lower than in the experiment (˜50%), the agreement in the details of the reconstructed spectra is excellent

- Motivation
- Brief FEL overview
- Description of the Experiment
- Experimental Results
- Time Domain Measurement
- FROG
- Conclusions

The Spectrogram of the pulse E(t)

$$S(\tau,\omega) = \left| \frac{1}{\sqrt{2\pi}} \int_{-\infty}^{\infty} E(t) g(t-\tau) e^{-i\omega t} \mathrm{d}t \right|^2$$

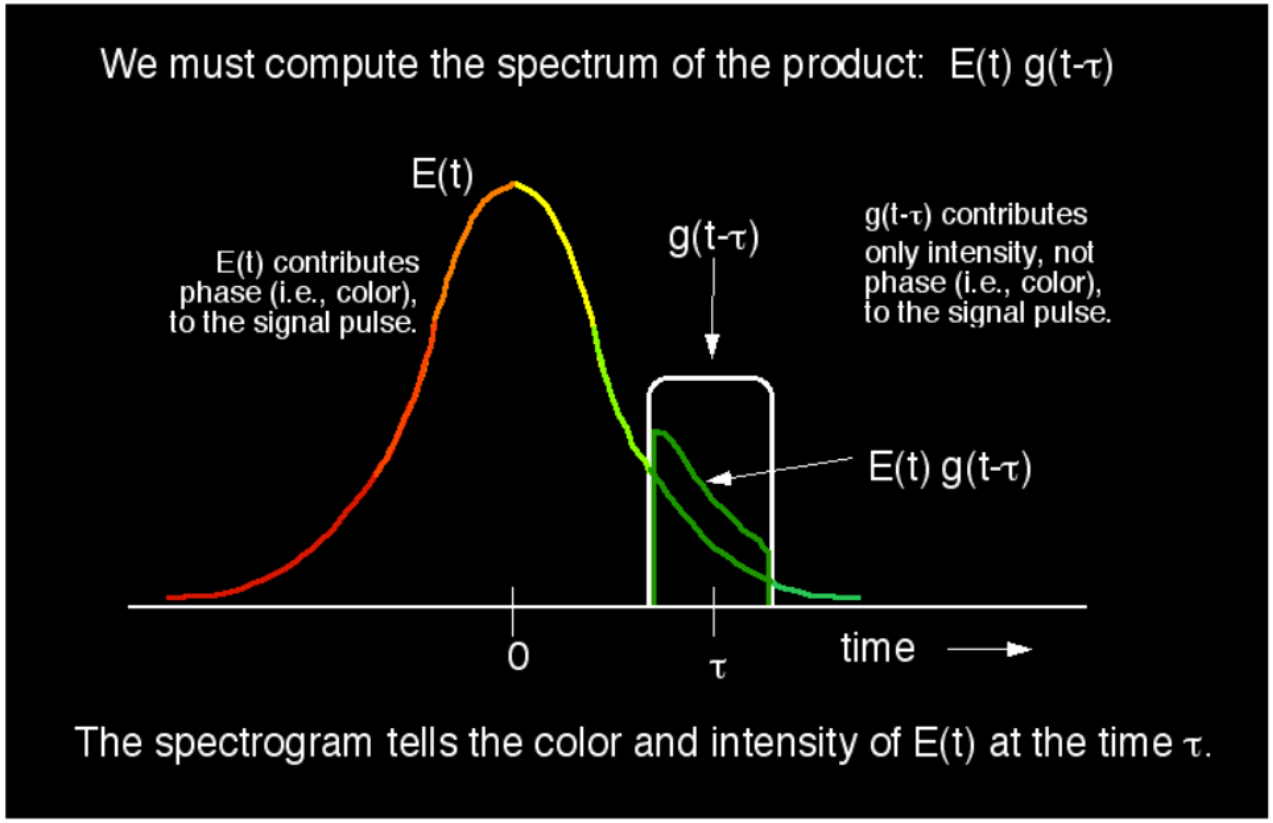

Trebino

Transient-Grating Frequency-Resolved Optical Gating

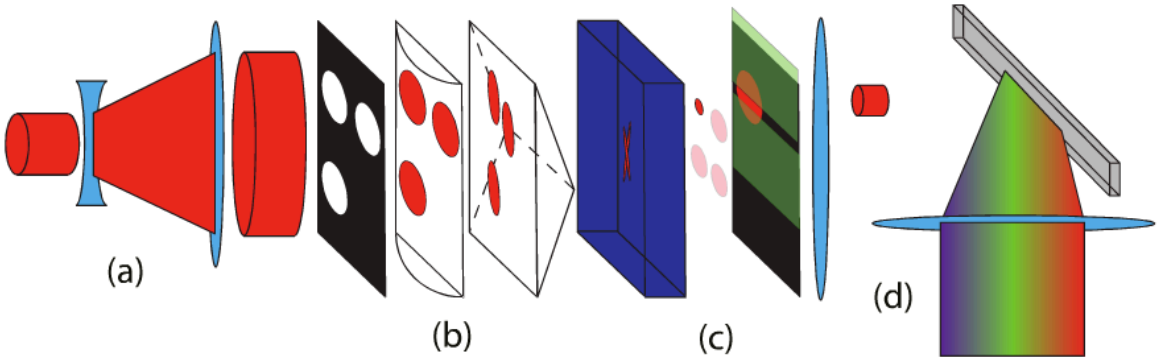

(a) beam expander; (b) input mask, cylindrical lens, Fresnel bi-prism; (c) nonlinear optical medium, output mask, knife edge slit; (d) Focusing optics, diffraction grating; (e) CCD camera

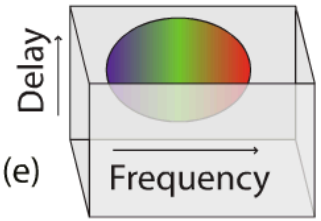

$$I_{FROG}^{TG} \propto \left| \int_{-\infty}^{\infty} E(t)|E(t-\tau)|^2 e^{-i\omega t} \mathrm{d}t \right|$$

- Advantages
  - Linear geometry
  - No additional delay lines
  - Works single-shot
  - No direction of time ambiguity
  - Broadband
  - Works into the UV
- Disadvantages
  - Third order nonlinear optical process
    - Requires high pulse power
  - Uses light off-axis
  - Scattered/Stray light

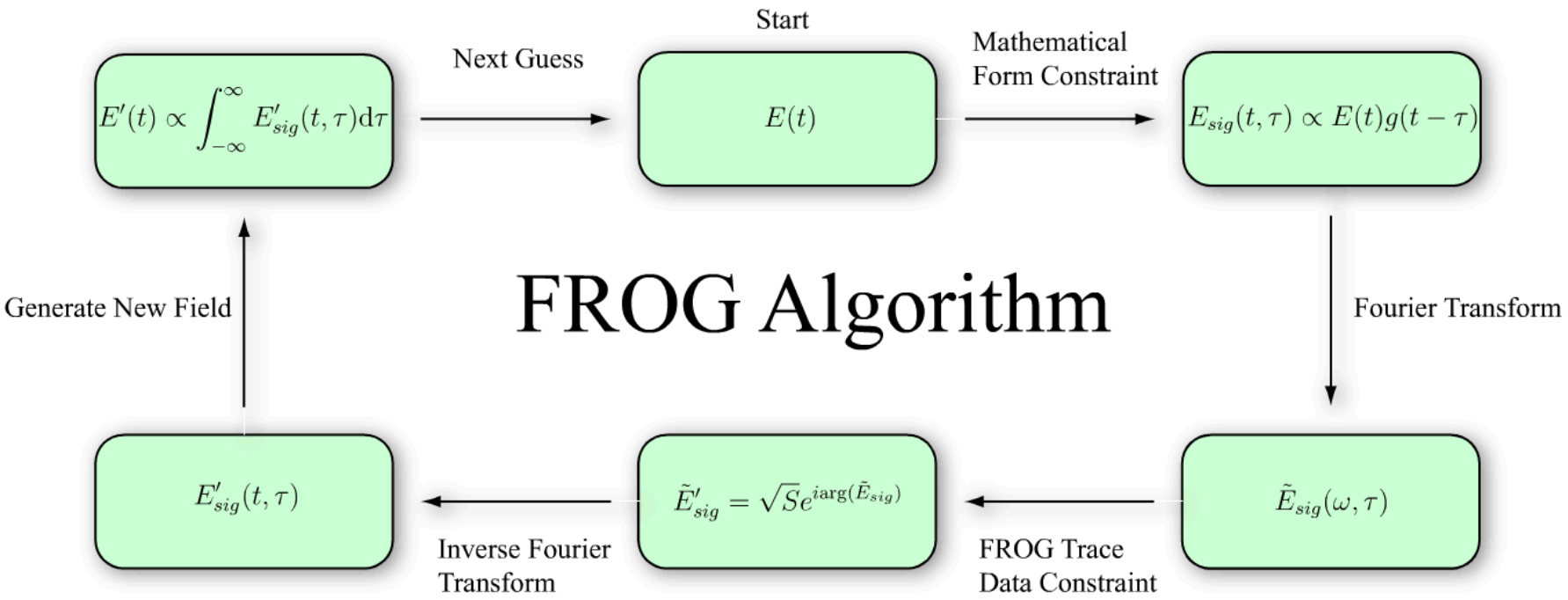
FROG Algorithm
Start
$E(t)$
Next Guess
$E'(t) \propto \int_{-\infty}^{\infty} E'_{sig}(t,\tau)\mathrm{d}\tau$
Mathematical
Form Constraint
$E_{sig}(t,\tau) \propto E(t)g(t-\tau)$
Fourier Transform
$\tilde{E}_{sig}(\omega,\tau)$
FROG Trace
Data Constraint
$\tilde{E}'_{sig} = \sqrt{S}e^{i\arg(\tilde{E}_{sig})}$
Inverse Fourier
Transform
$E'_{sig}(t,\tau)$
Generate New Field

Chirp/taper results - temporal domain I

Parameter	Symbol	Value
charge	Q	250 pC
current	I	264 A
e-beam energy	E	113.068 MeV
e-beam energy chirp	α	-2.484 keV/μm
rms slice energy spread	σ_γ	5×10^{-3} (Max)
normalized x(y) emittance	$\epsilon_{n,x(y)}$	2.27(1.6) mm-mrad
undulator period	λ_u	2.8 cm
nominal radiation wavelength	λ	530 nm

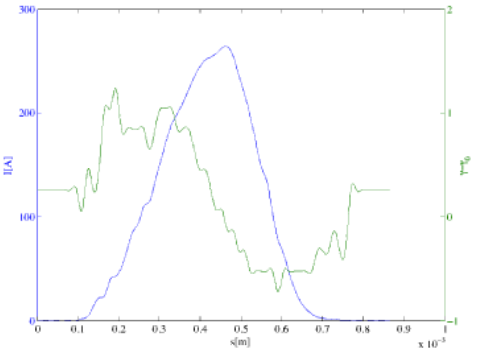

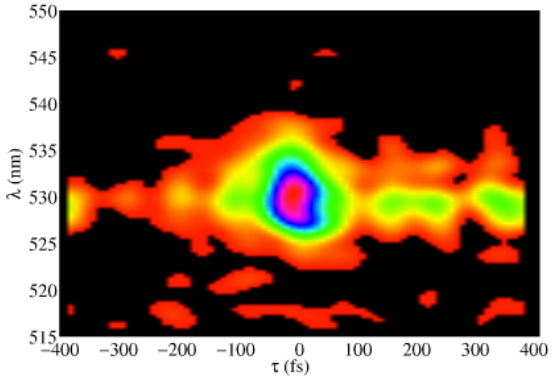

Experimental FROG trace

- Noise in the experimental trace
  - Algorithm can 'see through' the noise

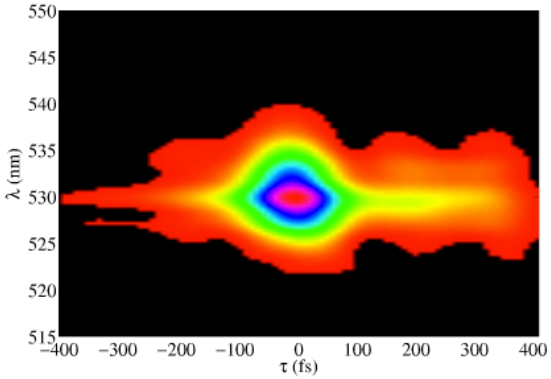

Reconstructed FROG trace

- Reconstruction and experimental traces show excellent overall agreement
  - Slight chirp
  - tail

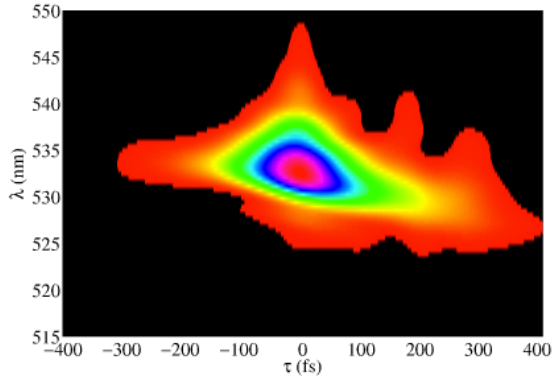

GENESIS FROG trace

- GENESIS FROG trace reproduces many of the features found in the experimental and reconstrcted traces

Chirp/taper results - temporal domain II

Transverse profile

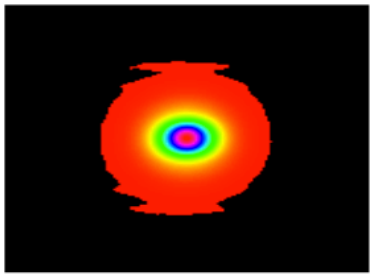

Transverse phase

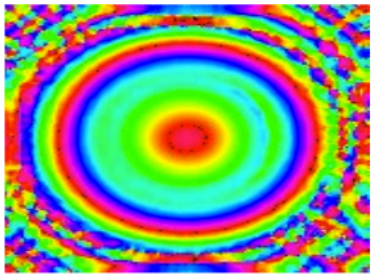

Power growth along the undulator

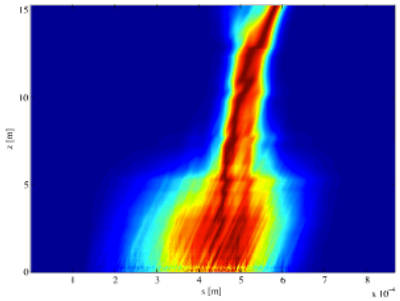

Reconstructed longitudinal profile

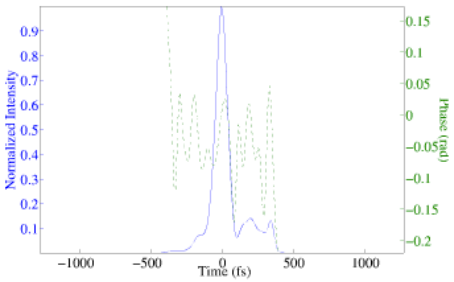

The dominant coherent spike has a pulse length:

$$\sigma_{\tau,FWHM} = 98fs$$

Off-axis GENESIS longitudinal profile

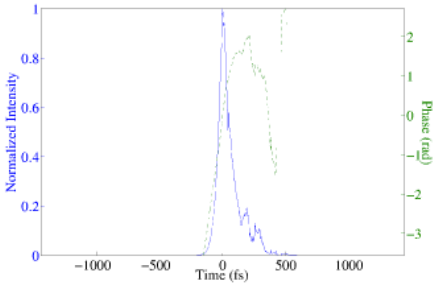

The off axis pulse length:

$$\sigma_{\tau,FWHM} = 91fs$$

Comparison between reconstructed, off-axis, and total longitudinal power

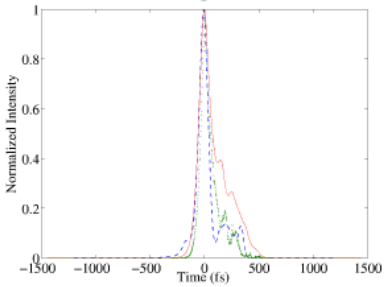

While the full power profile shows a more pronounced tail, the main features of the pulse are still captured by the off axis data gathered by the FROG

A rigorous determination of the time-bandwidth product for the reconstructed pulse yields:

$$\mathrm{TBP} = \tau_{rms}\omega_{rms} \sim 1.2$$

$$\omega_{rms}^2 = \int_{-\infty}^{\infty} E'(t)^2 \mathrm{d}t + \int_{-\infty}^{\infty} E(t)^2 \phi'(t)^2 \mathrm{d}t$$

Conclusions

- There are many users that are interested in controlling the longitudinal phase space of ultrafast pulses
- Methods exist to obtain single-spike pulses
  - Low charge, short e-beam
  - E-beam energy-chirp and undulator tapering
- Methods exist for measuring the phase space of optical pulses
  - FROG
    - TG FROG can potentially be used into the UV
- Future work
  - Extending FROG principles into ever shorter wavelength regimes